Coastal Dynamics 2017
Paper No. 185

DEPTH OF CLOSURE ALONG AN EMBAYED, MACRO-TIDAL AND EXPOSED COAST: A MULTI-CRITERIA APPROACH

Nieves Garcia Valiente[1], Gerd Masselink[2], Tim Scott[3] and Daniel Conley[4]

Abstract

The concept of depth of closure, denoted by DoC, is of fundamental importance in evaluating coastal sediment budgets, investigating shoreface morphodynamics, and in many coastal engineering applications. This key concept has been fully described in the literature, providing several approaches for its identification and parameterisation, but is not straightforward to apply to alongshore non-uniform macro-tidal coastlines. The overall objective of the present research is to apply different criteria to identify the active zone in the nearshore system, using as a study site the embayed, macro-tidal and high-energy coastline of North Cornwall and Devon (United Kingdom). Different approaches are implemented to identify the depth of closure, and theoretical and observational time-dependent interpretations are applied to assess DoC at the medium-term and on the regional scale.

Key words: depth of closure, shoreface, bed shear stress, extreme storms

1. Introduction

The concept of depth of closure (hereafter abbreviated to DoC) is of fundamental importance for the coastal engineering and management community. Indeed, the DoC is essential in many areas, e.g., for evaluating sediment budgets, investigating shoreface morphodynamics, identification of the active zone for beach nourishment design and dredge disposal, and for modelling coastal evolution. At some point offshore, hydrodynamic processes on the seabed will be sufficiently weak that depth changes over time are insignificant for a given purpose; the depth at this location is denoted as depth of closure (DoC), and is the subject of this paper. Of course, the definition of 'insignificant' is specific to the purpose, and thus different DoC criteria may be used to define the corresponding closure point. Most commonly, DoC is considered as the seaward limit of significant depth change for a specific period of time (Nicholls et al., 1998a, b). Thus, DoC is a morphodynamic boundary separating a landward active region, from a seaward inactive region (Hinton and Nicholls, 1998). Other authors consider the DoC similar to the depth beyond which wave-driven sediment transport is insignificant, and the term 'depth of no motion' is more appropriate (Phillips and Williams, 2007).

Several approaches have been pursued during the last four decades to estimate and quantify DoC. These can be synthesized in methods based on: wave characteristics (Hallermeier, 1981; Birkemeier, 1985; Capobianco et al., 1997); morphological data defining an envelope of variation that declines with depth (Hinton and Nicholls, 1998; Kraus et al., 1998; Nicholls et al., 1998a, b; Hartman and Kennedy, 2016; Ortiz and Ashton, 2016); and observations of sediment texture in sedimentary sequences (Roy and Thom, 1981; Thieler et al., 2001; Peters and Loss, 2012). Historically, DoC was estimated using profile comparisons as this enables direct estimation of the point at which no significant changes on the profile are detected, where 'significant' generally relates to bed-level change larger than the detection limit. This traditional method requires an extended dataset which is time-consuming and relatively expensive to

[1]School of Biological and Marine Sciences, Plymouth University, Drake Circus, PL4 8AA, Plymouth, UK.
nieves.garciavaliente@plymouth.ac.uk
[2]g.masselink@plymouth.ac.uk
[3]timothy.scott@plymouth.ac.uk
[4]daniel.conley@plymouth.ac.uk

obtain; therefore, direct estimates of DoC are only available from a small number of sites. The challenge in accurately quantifying DoC motivated the development of formulations to estimate DoC based on wave hydrodynamics (and sediment characteristics). Under the assumption that only the most energetic (i.e., largest) waves cause sediment transport out to the closure depth, Hallermeier (1978) developed an empirical approach to define two limits on the beach profile based on the activity experienced by the seabed: an inner and outer DoC. The inner limit DoC_1 represents the limit of significant morphological change and is defined as

$$DoC_1 = 2.28\, H_{12,t} - 68.5 \left(\frac{H_{12,t}^2}{g T_t^2}\right) \quad (1)$$

where DoC_1 is the predicted depth of closure over t years referenced to Mean Low Water (Hinton and Nichols, 1998); $H_{12,t}$ is the non-breaking significant wave height that is exceeded 12 hours over t years; T_t is the associated wave period; and g is the acceleration due to gravity. The outer limit DoC_2 denotes the limit of the shoal zone, representing the depth of no motion, and follows the expression

$$DoC_2 = \left(\overline{H_{s,t}} - 0.3\sigma_s\right)\overline{T_{s,t}} \left(\frac{g}{5000 D_{50}}\right)^{0.5} \quad (2)$$

where $\overline{H_s}$ is the annual mean significant wave height, σ_s is the associated standard deviation, $\overline{T_s}$ is the average significant wave period, and D_{50} is the grain size (in m). Both Eq. 1 and Eq. 2 have been shown to provide an accurate depth of closure on micro-tidal, wave-dominated, sandy coasts (Nicholls et al., 1996, 1998a, b). In the case of macro-tidal beaches, these depths should be considered relative to the average low spring tide level (Nicholls et al., 1998a, b). Although wave-based formulations are a common and widely-accepted approach to estimate DoC, it is appropriate to evaluate their usefulness in areas where geological control, as well as other hydrodynamic processes such as tidal currents, play an important role in terms of sediment dynamics on the shoreface.

Here, we apply a multiple-criteria approach to estimate DoC for the embayed, macro-tidal and high-energy coast of North Cornwall and Devon, described in Section 2. In Section 3, we estimate DoC based on morphological and sedimentological observations, and relate these to the wave-based theoretical approaches proposed by Hallermeier (1981) and Kraus et al. (1999). As the DoC concept aims to provide a limit for the active zone in the nearshore system, we then combine the methods to estimate DoC with wave-induced bed shear stresses modelled across our study domain. The modelled bed shear stresses are computed using the extreme wave conditions that define DoC to help understand the sediment movement limits (sediment motion, ripple formation and ripple destruction) within our study area. In Section 4, we explore the results of the different DoC formulations and discuss its replicability and application for geologically-constrained coastal areas. Finally, conclusions are presented in Section 5.

2. Study area

The North coast of Cornwall and Devon is located in the southwest of England (United Kingdom). The physiography of this coast can be considered as highly diverse, combining high hard rock cliffs with relatively short (< 5 km) embayed beaches, often backed by dune systems and cliffs, and separated by rocky headlands and small estuaries (Buscombe and Scott, 2008). The medium resistance to erosion of the cliffs combined with the main phases of transgression have resulted in a large proportion of embayed beaches that cover a wide spectrum from reflective to dissipative morphodynamic conditions. The configuration of the inner shelf is very diverse and includes large and deep bays with several beaches/embayments with varying orientations (Region 1 and 2; Figure 1); stretches of coast characterized by a relatively steep and narrow shoreface with shallow and mainly west-facing embayments separated by headlands (Region 3, 4 and 6; Figure 1); and sections with rocky cliffs fronted by sandy beaches, without any clear embayments (Region 5; Figure 1).

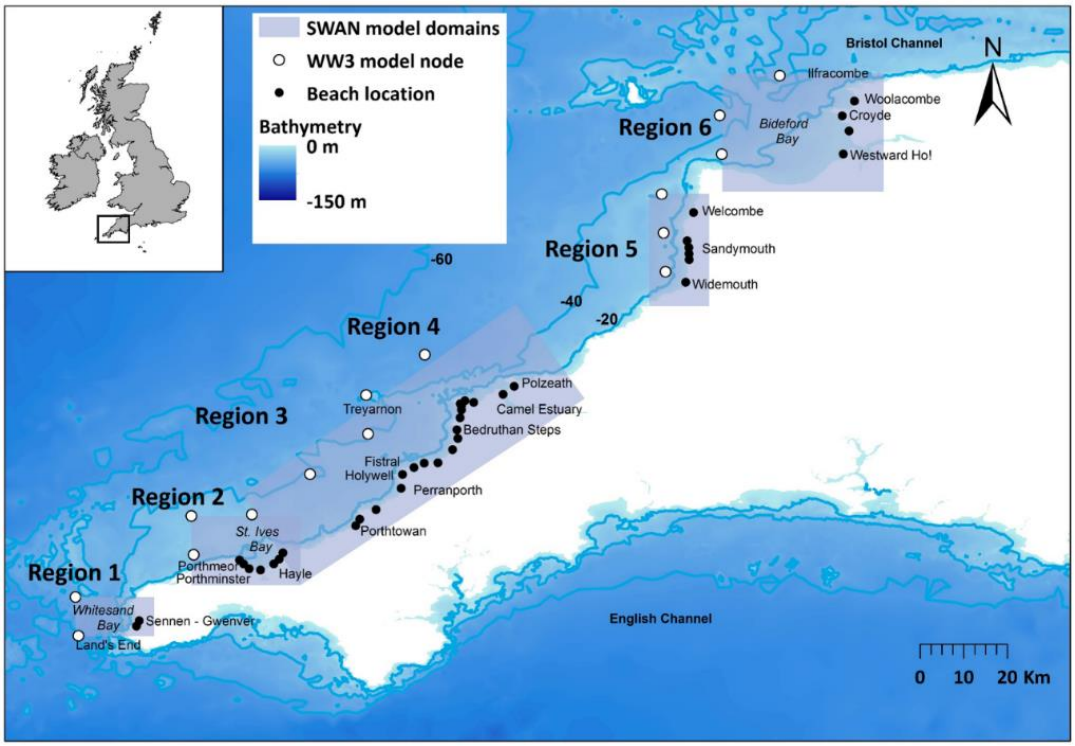

Figure 1. Map of SW England showing location of the six regions (grey shaded rectangles) considered relatively similar in terms of coastal configuration. The black dots in each of the regions represent the different study sites (N = 38) and the white circles represent the nodes used for the SWAN wave modelling

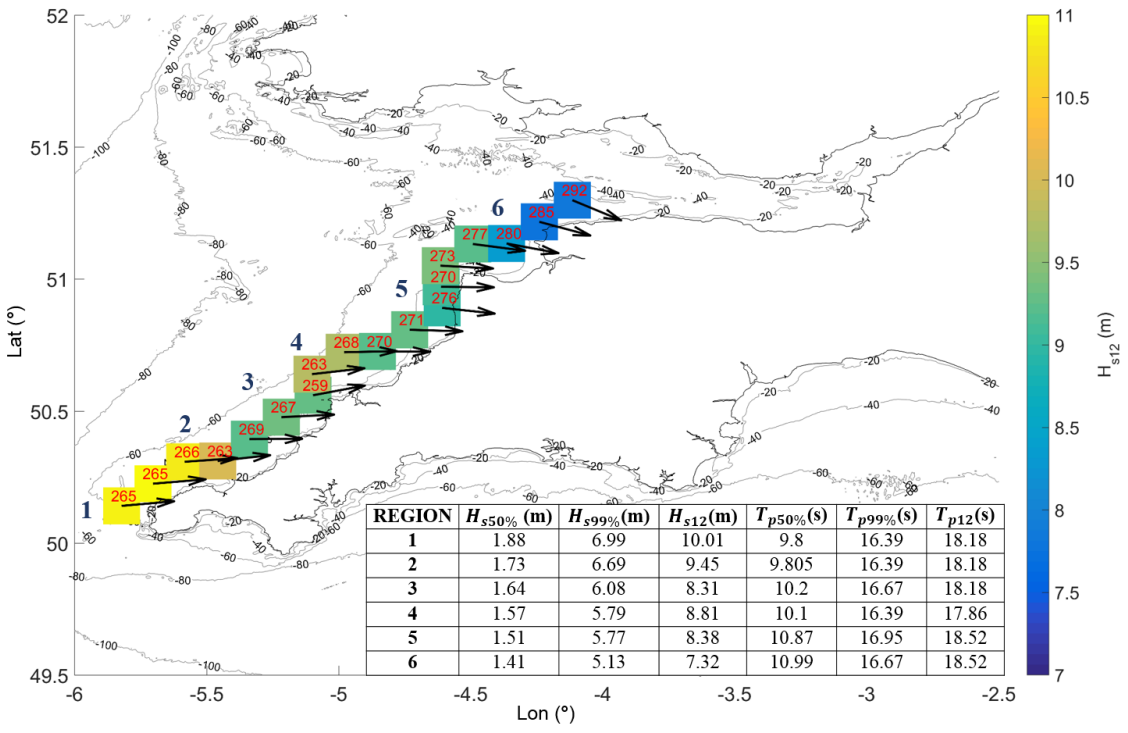

REGION	$H_{s50\%}$ (m)	$H_{s99\%}$ (m)	H_{s12} (m)	$T_{p50\%}$ (s)	$T_{p99\%}$ (s)	T_{p12} (s)
1	1.88	6.99	10.01	9.8	16.39	18.18
2	1.73	6.69	9.45	9.805	16.39	18.18
3	1.64	6.08	8.31	10.2	16.67	18.18
4	1.57	5.79	8.81	10.1	16.39	17.86
5	1.51	5.77	8.38	10.87	16.95	18.52
6	1.41	5.13	7.32	10.99	16.67	18.52

Figure 2. Spatial variability of offshore H_s exceeded 12 hours a year and direction along the coast of SW England obtained using the Met Office WW3 regional model wave data output from 2012 to 2016. Bottom right table shows deep water wave climate statistics for the selected regions (dark blue numbers indicate regions) from 2012 to 2016

The coastline of SW England is macro-tidal with the mean spring tide range varying between 6 m and 8 m (Scott et al., 2011). Tidal currents with values of 0.7 m s^{-1} have been recorded during spring tides near headlands and exceed 1 m s^{-1} in the Bristol Channel (unpublished data). Wave statistics for the different regions, based on 4 years (2012–2016) of modelled wave data from the Met Office 8-km WW3 wave model, are summarized in Figure 2. Statistics were computed for each WW3 node and averaged between the relevant nodes for each region of study. Wave conditions along the coast are characterized by energetic waves from the W and WNW quadrants as a result of a combination of Atlantic swell and local wind waves. There is a progressive change in the wave conditions from south to north: modal (50% exceedance) and extreme (99% exceedance) wave heights decrease ($H_{s50\%}$ from 1.9 m to 1.4 m; $H_{s99\%}$ from 7.0 m to 5.1 m), and the wave direction changes from W to WNW. The wave period is relatively constant along the coast ($T_{p50\%}$ = 10–11 s; $T_{p99\%}$ = 16–17 s). For the computation of DoC, the wave height that is exceeded 12 hours a year (and its associated period) is required (Eq. 1) . These extreme conditions are always associated with W sea states characterized by H_{s12} from 10.0 m in the south to 7.3 m in the north, with a similar period of T_{p12} = 18 s along the coast (Figure 2).

3. DoC estimation

There are numerous approaches for estimating DoC . Here we focus on those based on wave hydrodynamics as well as morphological observations covering a total of 5 criteria to identify DoC (Figure 3). The 4-year modelled wave data time series was used to extract mean and extreme wave conditions to compute inner (Eq. 1) and outer (Eq. 2) DoC based on the wave-based formulations of Hallermeier (1979, 1981). $H_{s,12}$ and its associated $T_{p,12}$ were transformed to shallow waters using SWAN and DoC_1 was calculated applying Eq. 1. Following Soulsby (1997), the transformed wave conditions were also used to compute the spatial distribution of the bed shear stress induced by the most extreme wave condition ($H_{s,12}$ and $T_{p,12}$). These were used to identify the depth boundaries where the modelled bed shear stress exceeds critical bed shear stress required for sediment transport and bedform activity. All approaches were applied to the six different regions shown in Figure 1, covering a total of 38 beaches (25 low tide embayments, LTEs) and 164 representative cross-shore profiles.

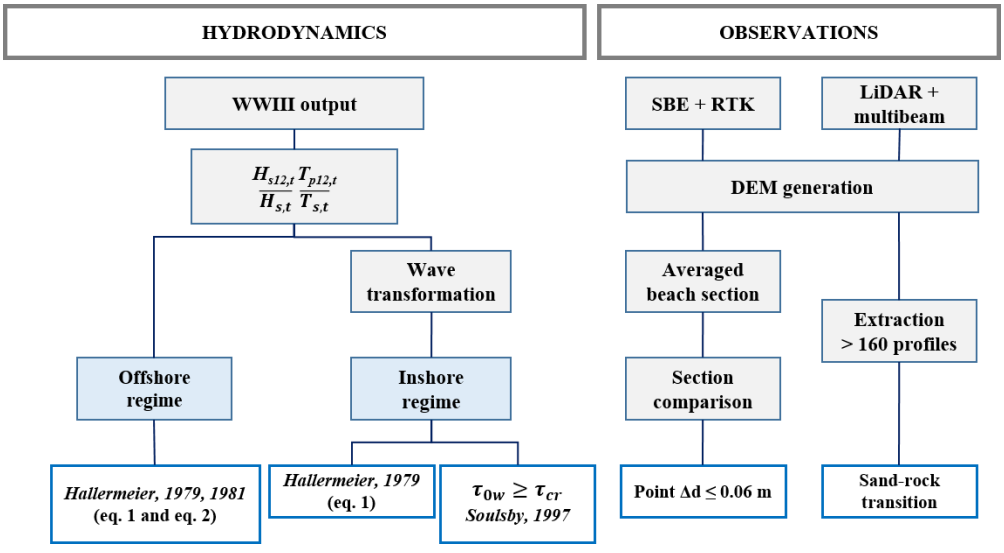

Figure 3. Flow diagram of research methodology of the DoC identification

For the application of the observational approaches we use 2 different datasets: (1) bathymetry data (provided by the United Kingdom Hydrographic Office, UKHO) for the offshore profile and LiDAR data (provided by Plymouth Coastal Observatory) for the upper beach covering the entire SW coast; and (2) seasonal single beam and RTK survey datasets from 2007 to 2016 for the beach of Perranporth (Region 3).

In both cases, the datasets were merged to produce different Digital Elevation Models (DEM). The DEM of the SW was used to extract 164 profiles (up to -30 m ODN) representative of the different study sites, where the transition point between sand and rock was identified based on the smoothness and/or the break in the shape of the shoreface profiles. Perranporth DEMs were used to develop profile comparison, to enable identification of the point at which morphological change can be considered insignificant ($\Delta d \leq 0.06$ m). A flow diagram that synthetizes the methodology followed to develop the study is presented in Figure 3.

Four years (2012–2016) of modelled wave data output from the 8-km resolution regional wave forecast model (based upon the NCEP community model WAVEWATCH III, WW3) (see Figure 1 for WW3 output locations) was used to analyze temporal and spatial variability of wave climate along the coast (presented in Section 2). This wave data series includes the winter of 2013–2014, which represents the most energetic winter over the last 7 decades (Masselink et al., 2015), making the model output suitable to estimate DoC. Modelled wave data was used to compute Hallermeier's wave-based formulations (Eqs. 1 and 2) applying the extreme (Eq. 1) and mean (Eq. 2) regime statistics extracted from each relevant WW3 node. Both DoC_1 and DoC_2 were computed for the total time series (t = 4 years), as well as independently for each of the years (t = 1 year) and then averaged ($\langle DoC_1 \rangle$ and $\langle DoC_2 \rangle$).

Offshore wave conditions are not necessarily representative of inshore wave conditions within deep embayments and/or on coastlines that do not face into the prevailing wave direction. Therefore, the DoC computed using these offshore conditions may not be appropriate and a wave refraction model was used to transform offshore wave conditions to the nearshore. For each of the six regions the modelled wave data were ordered into seven different wave direction classes: 165–195°, 195–225°, 225–255°, 255–285°, 285–315°, 315–345° and 345–15°. For each of these classes, the wave heights were ranked, and the $H_{s12,t}$ and associated $T_{p12,t}$ were selected (for t = 4 and t = 1 year). The third-generation spectral wave model SWAN (Booij et al., 1999) was used to transform these extreme wave conditions from offshore to inshore. SWAN was set up for five different domains (one for each region, except Regions 3 and 4 which had a shared domain; refer to Figure 1) with a grid resolution of 100x100 m, so wave height values could be allocated to each embayment in the regions. Following Kraus et al. (1998), wave height and the associated period were determined at a nearshore location (from 20 to 12 m depth) and substituted in the wave empirical formulation of Hallermeier (Eq. 1). Maximum values of the maximum DoC_1 for each of the direction classes were selected at these locations. Finally, to obtain a unique DoC_1 and $\langle DoC_1 \rangle$ value for each embayment, DoC was alongshore-averaged. In order to reference to the same datum, a correction from MLWS to ODN was applied (based on MLWS for macro-tidal settings).

A more process-based approach to the DoC concept, as opposed to the parametric approach of Hallermeier (1978, 1981), is to quantify the bed shear stresses τ_{0w} on the sea bed under extreme wave conditions and compare these to sediment motion thresholds τ_{cr}. The methodology proposed by Soulsby (1997; see pages 65–110) is used here. To compute the potential for wave-induced sediment resuspension, the root-mean square value of the orbital motion velocity

$$U_{rms} = \left(\sum_{i=1}^{N} U_i^2 \right)^{1/2} \tag{3}$$

was computed using SWAN through the expression

$$U_{rms}^2 = \int_0^{2\pi} \int_0^{\infty} \frac{\sigma^2}{\sinh(kd)^2} E(\sigma, \phi) \mathrm{d}\sigma \mathrm{d}\phi \tag{4}$$

where d is water depth, k is the wave number, σ is the angular frequency, and $E(\sigma, \phi)$ is the spectral density. Wave induced shear stress τ_{0w} was obtained using the expression

$$\tau_{0w} = \frac{1}{2} \rho f_w U_w^2 \tag{5}$$

where f_w is the wave friction factor and $U_w = \sqrt{2} U_{rms}$. The wave friction factor for turbulent flow depends

on the bed roughness ($z_0 = D_{50}/12$) and the semi-orbital excursion ($A = U_w T/2\pi$) as follows

$$f_{wr} = 1.39\left(\frac{A}{z_0}\right)^{-0.52} \tag{6}$$

Soulsby (1997) relates sediment motion threshold for a specific seabed with the critical Shields parameter θ_{cr} through the expression

$$\tau_{cr} = \theta_{cr} g(\rho_s - \rho) D_{50} \tag{7}$$

where ρ_s is the sediment density, D_{50} is sediment size and g is the gravitational acceleration.

According to Eqs. 6 and 7, initiation of motion, as well as sediment transport, will depend on boundary shear stresses and seabed characteristics. Based on laboratory experiments and observations, Nielsen (1981) argued that the occurrence of bedforms is related to the bed shear stress (τ_{0w} or θ) and developed a relation between bedform type and wave energy conditions, expressed as a function of transport stage. Using Grant and Madsen (1982), and considering a seabed composed by medium sand D_{50} = 0.3 mm, the following critical values of the Shields number (θ_{cr}) can be identified: (1) initiation of motion θ_{cr}= 0.048; (2) formation of sharp-crested vortex ripples θ_{cr} = 0.1; transformation from vortex to post-vortex ripples θ_{cr} = 0.2; and transition into a plane bed θ_{cr} = 1. Following Eq. 7, wave-induced bed shear stress was computed for each region, and compared with the critical shear stress τ_{cr} for the different scenarios.

The final approach to estimating DoC involves the comparison of multiple topographic profiles (alongshore-average of 110-m section) collected over several years for the dissipative sandy beach of Perranporth (located in Region 3; refer to Figure 1). This morphological data was generated using combined field measurements of RTK topographic and single beam datasets from 2007 to 2016, providing a time series long enough to obtain a relevant comparison with the wave-based theoretical methods tested.

4. Results

4.1 *Closure depth computed using offshore wave conditions*

All DoC results computed using offshore waves have been summarized in Figure 4 with the bars comprising the different regions (refer to Figure 1). To be consistent across the different regions, and other studies, the DoC values are related to MLWS (application of Eqs. 1 and 2 for macro-tidal coastlines) and then converted to ODN, which is the vertical datum used in the UK (c. 0.2 m above MSL in the SW of England). DoC_1values decrease from 23.3 m in the south (Region 1) to 18.8 m in the north (Region 6) when the extreme wave condition ($H_{s,12}$ and $T_{p,12}$) over the 4-year data set is used, but values are c. 4 m less when $\langle DoC_1 \rangle$ is computed. Values of the outer depth of closure DoC_2 are c. 50% greater than the inner value DoC_1 for all the regions of study, with values decreasing from 50.1 m in the south to 33.6 m in the north and from 47.2 to 30.7 m for $\langle DoC_2 \rangle$. The largest closure depths are registered for the 2014 as the largest wave conditions were experienced during this winter. In all cases, depth of closure values (DoC_1 and DoC_2) decrease from south to north in response to the associated decrease in the wave conditions (refer to Figure 2).

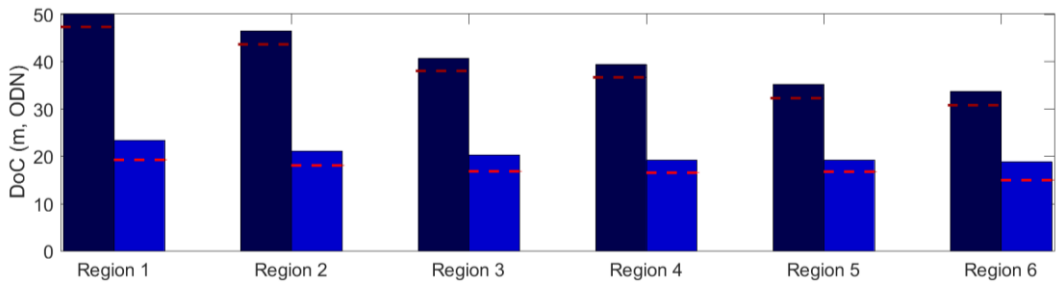

Figure 4. Computed depth of closure at each region obtained by applying the Hallermeier inner and outer DoC formulations using offshore WW3 wave conditions. Dark blue bars are DoC_2 values and light blue bars correspond to DoC_1. Red dashed lines across bars represent $\langle DoC_2 \rangle$ (dark red) and $\langle DoC_1 \rangle$ (light red)

4.2 *Spatial variability in closure depth due to wave refraction/diffraction in embayments*

The offshore wave conditions in c. 40-50 m are not necessarily representative of the inshore wave conditions, particularly for the more embayed locations and/or where the coastline is not directly facing the prevailing wave direction. In this case, wave refraction/diffraction around headlands is likely to generate a significant gradient in the wave height and thus a spatial variability in the depth of closure. The offshore waves were therefore transformed into intermediate and shallow water depth, and, following Kraus et al. (1999), the depth of closure DoC_1 was computed using the wave conditions at different contour lines, in our case for the 12–20 m depth contours (relative to ODN) at 1-m intervals. This yields DoC_1 values that vary both along and across the embayment, and, as an example, the spatial variation in DoC_1 for Region 2 is presented in Figure 5. DoC_1 varies most widely in embayments that display a considerable difference in their orientation and for the case of Region 2 the more exposed sections are characterized by higher DoC_1 values (> 10 m) than the more sheltered sections (< 8 m). The results for Region 2 are representative of other regions with considerable variability in shoreline orientation and/or with important points of refraction (e.g., Regions 4 and 6). Typical values of DoC_1 for the most exposed parts of the coast (Regions 1 and 6, and the north part of Regions 3 and 4) are 12–16 m (relative to ODN), whereas DoC_1 values for the more sheltered parts (Regions 2 and 5, and the south part of Region 6) are typically 6–10 m. Most importantly, the depth of closure values DoC_1 based on inshore wave conditions are significantly smaller than those based on offshore wave conditions.

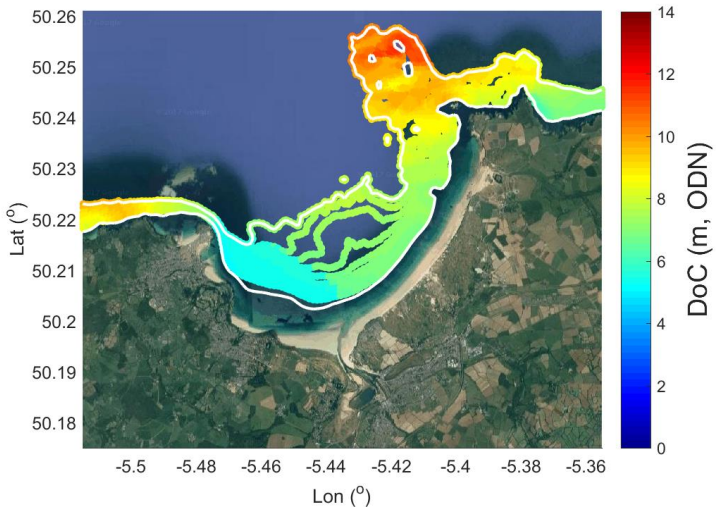

Figure 5. Depth of closure computed following Kraus et al. (1999) in Region 2. DoC_1 has been estimated using the offshore $H_{s,12}$ and $T_{p,12}$ propagated to nearshore waters using the SWAN model and subsequently computed at the contour lines from 12 to 20 m depth using the wave-based formulation (Eq. 1) of Hallermeier (1981). The white lines represent the 14- and 20-m contour lines

4.3 *Embayment-averaged closure depth*

The spatial variability in DoC_1 for each region, such as presented in Figure 5, is considered an improvement to simply using the offshore wave conditions, especially for the more embayed regions. However, having to derive a single depth of closure value from Figure 5 is not practical. To obtain an estimate of the depth of closure for each of the 25 embayments, all DoC_1 estimates along each embayment, computed using Eq. 1 and based on the wave conditions modelled for the 20-m contour line, were averaged and are plotted in Figure 6. DoC_1 values are very variable and range from 8.9 m at Porthmeor and Porthminster (relatively small and NE-facing embayments in Region 2) to 16.2 m in Polzeath and 16.8 m at Bedruthan Steps (larger and W-facing embayments in Region 4). It is evident that exposure plays a key role in explaining the spatial variability in the depth of closure. DoC_1 for the case of Region 3 varies from 13.7 m (embayments in the centre of the region) to 16.8 m in the open W orientated embayments of Region 4. Embayments in Region 2 are affected by an important point of refraction as St. Ives head and present

values of DoC_1 increasing from 8.9 to 10.2 m, from W to E, as exposure increases. In Region 5, which is characterised by a relatively straight coastline with no prominent embayments, the closure depth is alongshore uniform and only ranges from 10.4 m to 10.6 m. Generally, the largest within-embayment variability in DoC_1 (length of the red vertical lines in Figure 6) occurs in the larger embayments (e.g., Sennen – Gwenver; Camel Estuary – Polzeath), whereas limited variability in DoC_1 occurs in the smaller embayments (e.g., Porthmeor, Crantock, Porthcothan, most embayments in Region 5).

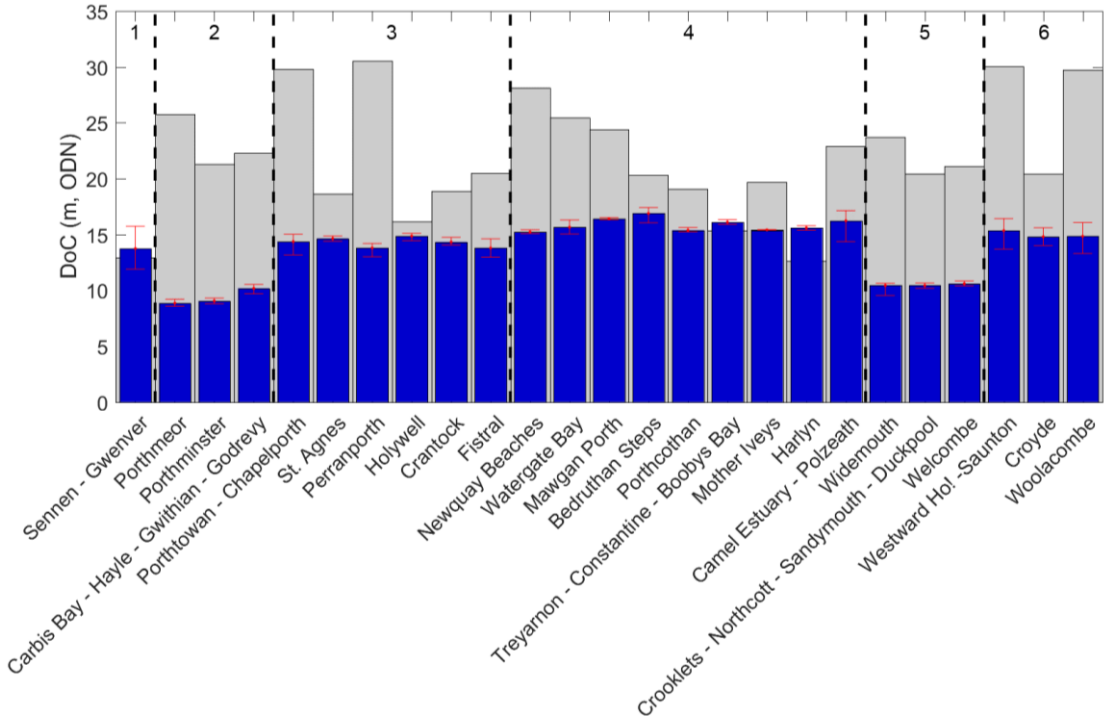

Figure 6. Along-coast variability in depth of closure. Blue bars represent the average DoC_1 for each embayment, computed using the modelled inshore wave conditions at the 20-m contour line and forcing the SWAN wave model with $H_{s,12}$ and $T_{p,12}$ derived from the 4-year time-series. Minimum and maximum DoC_1 values for each embayment are represented by the red intervals. Grey bars correspond with the embayment-averaged depth of the transition between sand and rock. Black dashed lines separate the embayments of each region (the number of the corresponding region is indicated in the upper part of the panel)

The average depth of the transition between sand and rock for each of the embayments is also plotted in Figure 6 and comparison between DoC_1 indicates a good correspondence for Sennen Cove, Hollywell and Treyarnon; all cases where the rocky platform appears at shallower depths. For the other embayments, the depth of the sand/rock transition, which ranges from 15 m to 30 m, is significantly deeper than the DoC_1; frequently more than twice the depth (e.g., for Porthmeor, Perranporth, Widemouth, Woolacombe).

4.4 *Observed closure depth at Perranporth*

Survey (beach and bathymetry) data from Perranporth (Region 3) is analyzed to derive the actual closure depth for this location. Figure 7 shows the mean and the envelope associated with all alongshore-averaged shoreface profiles for Perranporth collected over the period 2010–2016. The location on the profile with the largest bed-level variability (0.5 m) corresponds with the outer bar region (x = 700–900 m). The vertical variability decreases to less than 0.06 m (according to Nicholls et al. (1998a) 0.06 m is equivalent to the estimated error in Hallermeier Eq.1) at the depth of -14.8 m (ODN) and this is considered the depth of closure for this embayment.

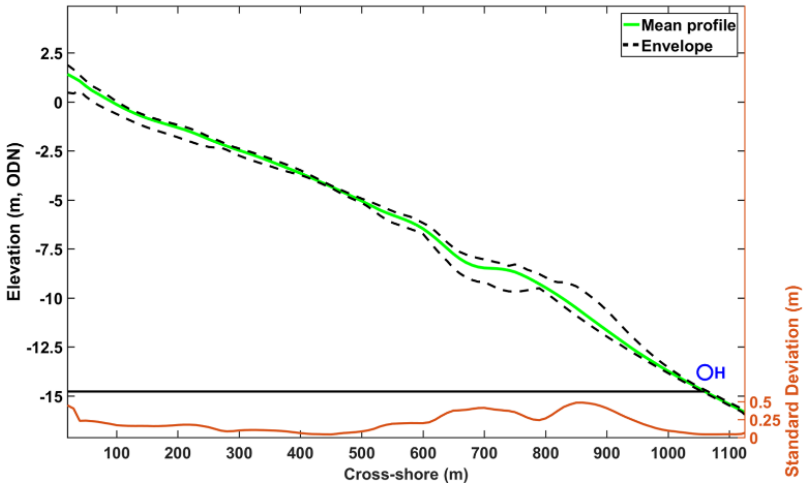

Figure 7. Observed depth of closure estimated for Perranporth beach, north Cornwall, from: (1) the profile envelope (dashed black lines around the mean profile depicted by the green line; brown line representing the width of the envelope) and associated with beach survey data collected from 2010 to 2016. The blue marker 'H' represents the embayment-averaged DoC_1 computed using Hallermeier (1978) at the 20-m contour line and based on the most extreme wave conditions over the 4-year wave time series. The presented profile represents the alongshore-average profile of a 110-m wide section located in the south of the beach

The DoC_1 and $\langle DoC_1 \rangle$ values based on Eq.1 and offshore wave conditions for Perranporth are 20.2 m and 16.7 m, respectively. When the inshore wave conditions at the 20-m contour are used, the DoC_1 value decreases to 13.8 m, and the $\langle DoC_1 \rangle$ value to 13.4 m. This suggests that the offshore formulation over-predicts the closure depth.

4.5 *Wave-induced bed shear stresses under extreme wave conditions*

The output from the SWAN wave modelling for the most extreme wave conditions ($H_{s,12}$ and $T_{p,12}$) was used to compute the wave-induced bed shear stress τ_{0w} across all study regions (Figure 8). Values of τ_{0w} > 5 N m^{-2} occur at depths between 10 and 20 m in Regions 1, 3 and 6, which are predominantly west-facing embayments with a wide shoreface. Bed shear stress are significantly less (τ_{0w} < 1 N m^{-2}) at similar water depth off NE-facing beaches, such as Porthminster and Carbis Bay with a sandy flat shoreface in Region 2 (Figure 8; panel B). Interestingly, there are several other NE-facing embayments (e.g., Mother Ives and Harlyn in Region 4), that have similar values for τ_{0w} (c. 3.5 N m^{-2} in 28 m water depth) than the exposed west-facing embayments in Regions 1 and 3. This is attributed to the morphological configuration of these embayments, which are fronted by a short rocky shelf (c. 700 m) that limits wave energy dissipation during wave transformation and refraction.

The computed τ_{0w} values were compared to the following four sediment transport thresholds: (1) sediment motion τ_{cr}= 0.34 N m^{-2}; (2) initiation of vortex ripples τ_{cr} = 0.48 N m^{-2}; (3) initiation of post-vortex ripples τ_{cr} = 0.95 N m^{-2}; and (4) transition to upper plane bed τ_{cr} = 4.77 N m^{-2}. As evident from Figure 8, the first three sediment transport thresholds τ_{cr} are exceeded in all study region even a depths > 50 m.

The transition to upper plane bed varies considerably across all regions. For Region 1, this threshold occurs in depths > 30 m in the exposed northern part of the embayment, but decreases to c. 12 m at the more sheltered southern end, resulting in an average threshold of 25.5 m (Figure 8, panel A). In Region 2, the location of the upper plane bed threshold is spatially highly variable with significantly smaller values of c. 10 m at the southern end, areas where this threshold is not exceeded (e.g., Porthminster and Carbis Bay) and a more exposed section with values > 28 m (e.g., Godrevy and Gwithian). Embayment-averaged values for the transition depth are generally inflated due to the maximum transition depth values associated with the headlands, which often have values of c. 30 m. In the more alongshore-uniform Regions 3 and 4 (Figure 8, panels c and d, respectively), the isobath for the upper plane bed transition is 23 m and 25 m, respectively. Values for the embayments within these regions are generally around 18–20 m for Region 3

and close to 25 m for Region 4 (similar to the value around headlands), while around the headlands values are > 28 m. In Region 5, the depth for the transition to upper plane bed is restricted both around headlands and in the beaches to 12 m. Finally, in Region 6 (Figure 8; panel F) the transition depth closely follows the 20-m contour line (Saunton, Croyde and Woolacombe), and decreases to 10 m in the south of the region.

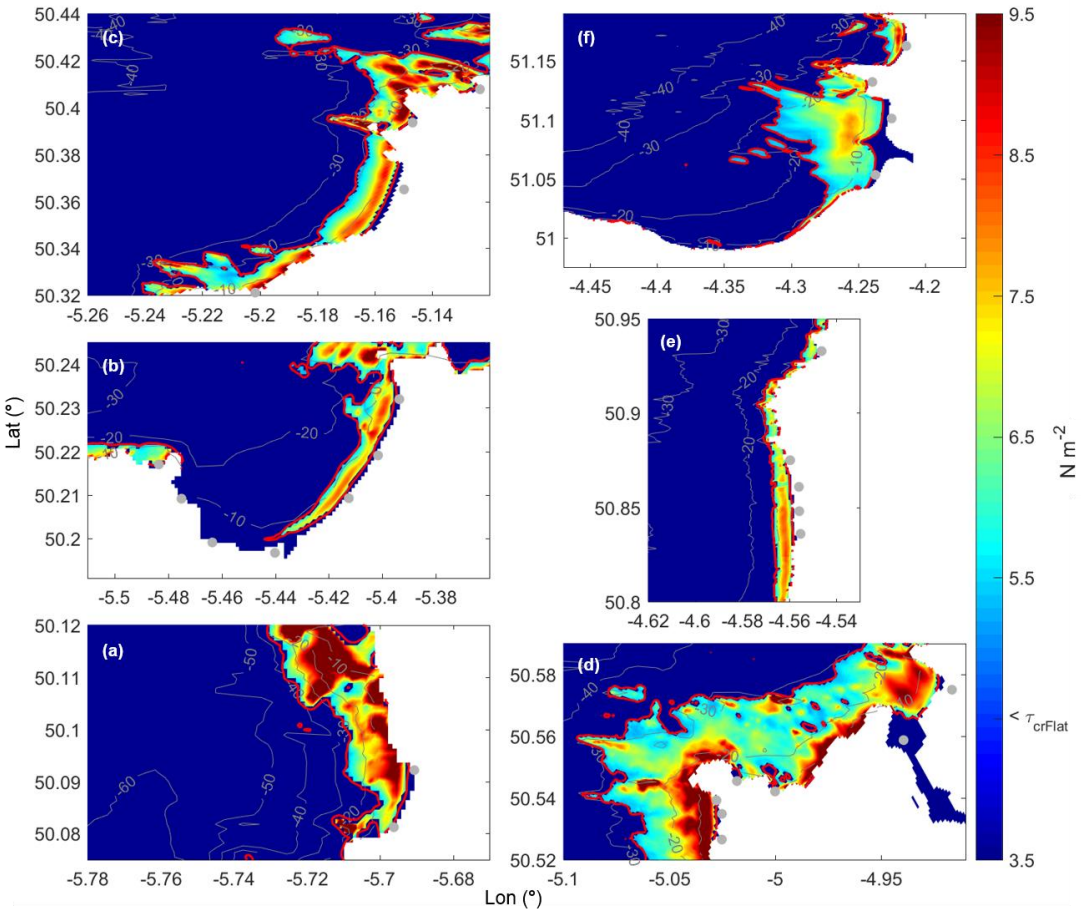

Figure 8. Wave-induced bed shear stress τ_{0w} computed for extreme wave conditions ($H_{s,12}$ and $T_{p,12}$) for all regions: (a)–(f) represents Regions 1–6. The red line represents the bed shear stress at the transition to upper plane bed conditions (τ_{cr} = 4.77 N m^{-2})

The DoC_2 values obtained using the offshore wave conditions (refer to Figure 3) are compared with the region-averaged upper plane bed transition depth. This average transition depth is reasonably representative for Regions 3, 4, 5 and 6, but conceals the large variability between headlands and embayments in Regions 1 and 2 (refer to Figure 8). DoC_2 results range from 50 m (southern region) to 34 m in Region 6, and the region-averaged upper plan bed transition depths are c. 40% smaller (decreasing from 25.5 m in Region 1 to 20 m in Region 6) suggesting that DoC_2 is not representative of the transition to upper plane bed conditions. When DoC_2 is compared with the other three sediment transport thresholds (sediment motion, initiation of vortex ripples and initiation of post-vortex ripples), the results indicate that the initiation of post-vortex conditions corresponds to DoC_2 best, whereas the initiation of sediment motion and formation of vortex ripples occurs at significantly larger water depths than DoC_2. This suggests that, in our study area, DoC_2 corresponds to the depth at which under extreme wave conditions post-vortex ripples develop and such bedform regime is characterised by significant sediment resuspension.

5. Discussion and conclusions

Depth of closure is a key concept to describe shoreface morphodynamics. It varies over time and space, and it is widely used to identify the active zone of the beach-shoreface system. Wave-based empirical

models used to estimate closure depth DoC are highly dependent on the timescale of interest, and are considered to yield good predictions for a medium-term timescale (1 to 4 years) in open, wave-dominated embayments (Nicholls et al., 1998a). In this study, different wave-based methods were used to compute DoC and compared with observations along the highly diverse and macro-tidal coast of north Cornwall and Devon. We used a 4-year time series of wave conditions, which included the most energetic winter affecting the coast of SW England (winter 2013/14) since at least 1948; therefore, the predicted DoC values can be considered to represent at least the decadal time scale.

The analytical model of Hallermeier (1991), expressed by Eq. 1, was applied to the six regions comprising 25 embayments on the north coast of Cornwall. Different approaches were followed in obtaining the closure depth DoC_1. Inserting offshore wave conditions into Eq. 1, as suggested by Kraus et al. (1998), resulted in DoC_1 values that were 20–50% larger than if inshore wave conditions were used. Using the latter is considered more appropriate along embayed coastlines, especially for sites where headlands are a key factor in controlling the inshore wave conditions (e.g., Porthminster and Carbis Bay in Region 2 and Mother Ivey's and Harlyn in Region 4). However, the closure depth computed using the inshore wave conditions depends on the water depth from which the wave height is extracted: the shallower the depth, the smaller the waves, and the lower the DoC_1 value. The inshore wave height at 20 m water depth was used here. Another consideration is the time period over which to determine the extreme wave conditions. If $H_{s,12}$ and $T_{p,12}$are derived from the complete wave time series (4 years in the present case), the DoC_1 values are c. 4 m larger than if $\langle DoC_1 \rangle$ is used (yearly-averaged DoC_1 computed using $H_{s,12}$ and $T_{p,12}$ for each year in the time series). As the depth of closure concept generally related to shoreface variability over inter-annual to decadal time scale, it seems appropriate to select the longest time series possible to estimate DoC_1.

The cross-shore distribution of the seabed composition can be used to help identify limits of cross-shore sediment exchange (Roy and Thom, 1981; Thieler et al., 2001; Peters and Loss, 2012). For lack of information on the cross-shore variability in sediment characteristics, we focus here on the transition between sand and rock, based on the shape of the shoreface profile (smooth versus rough). The sand-rock transition depth is not necessarily related to the closure depth, but it can add value when following a multi-criteria approach to determine DoC, especially where the closure depth obtained from analytical methods is located landward of the sand-rock transition depth. As this was only the case in 3 of the 25 embayments, this suggests that despite the rocky nature of the coastline of North Cornwall, there is sufficient sediment present on the shoreface of most embayments to enable development of an equilibrium shoreface profile.

Morphological methods based on observations are the most accurate tool to estimate DoC; however, they are logistically demanding to obtain, requiring both time and considerable funding, restricting its application to a reduced number of sites. For the case of Perranporth, our results show a most active zone of up to 14–15 m water depth (relative to ODN). It is concluded that the value for the closure depth for Perranporth is correctly estimated using Hallermeier (1991) Eq. 1 provided: (1) $H_{s,12}$ and $T_{p,12}$ are computed using the wave time series that encompasses the shoreface monitoring period; (2) the offshore wave conditions are transformed into intermediate/shallow water; (3) the modelled inshore sea state at the 20-m contour line in several representative profiles of the embayment is inserted into Eq. 1 and the embayment-averaged closure depth is computed; and (4) the depth of closure value is considered relative to MLWS and then corrected to the survey datum (ODN for the case of the UK).

Bed shear stress studies contribute to a better understanding of the depth of closure as a theoretical boundary for sand motion, corresponding to a seaward limit of the 'wave-constructed' profile (Hallermeier, 1981) and thus the outer depth of closure limit DoC_2. Bed shear stress values at the transition to upper plane bed occur at depths > 20 m in most cases and are c. 40% smaller than the DoC_2 values computed using Eq. 2. The wave orbital velocities across the shoreface computed for most extreme waves suggest that under such conditions most of the embayments experience extreme sediment motion up to large depths. Computed bed shear stresses suggest that along the north coast of Cornwall, extreme wave events induce sediment entrainment, vortex ripple formation and post-vortex ripple formation, and thus sediment resuspension, across the entire study domain at water depths > 40 m. The transition to upper plane bed occurs around the 20–26 m isobaths for the most exposed embayments (e.g., Regions 1 and 3), suggesting that wave currents during an event of the characteristics of the 2013/14 winter storms can induce sediment transport well seaward of the limit where calm conditions will be able to return the sediment as part of the recovery process. Recent research into this topic suggests that some of the embayments along the north coast have recovered > 50% since the 2013/2014 storms, while other embayments, such as Sennen (Region

1) and Perranporth (Region 3) have recovered significantly less (Burvingt et al., 2017). The considerable depth at which wave-driven sediment transport is likely under extreme wave conditions, easily > 40 m depth and a considerable distance seaward of the headlands, also challenges the notion of embayments being closed sediment cells in the SW of England as suggested by May and Hansom (2003). A re-evaluation of the concept of closed embayments is especially appropriate for the north Cornish coastline as, in addition to the wave-exposed setting, maximum tidal currents around headlands are considerable (c. 0.7 m/s); therefore, wave/current interaction under energetic waves during spring tide conditions are expected to result in significant sediment fluxes at water depths > 20 m.

Acknowledgemets

This work was supported by UK Natural Environment Research Council (NE/M004996/1; BLUE-coast project).

References

Birkemeier, W.A., 1985. Field data on seaward limit of profile change, *Journal of Waterway, Port, Coastal and Ocean Engineering*, 111(3): 598-602.

Booij, N., Ris,R.C. and Holthuijsen, L.H., 1999. A third generation wave model for coastal regions, part I, model description and validation, *Journal of Geophysical Research*, 104(C4): 7649–7666.

Burvingt, O., Masselink, G., Russell, P., Scott, T., 2017. Beach evolution and recovery from a sequence of extreme storms, *Proceedings Coastal Dynamics*, ASCE, Helsingor, Denmark, this volume.

Buscombe, D.D. and Scott, T., 2008. The coastal geomorphology of north Cornwall, Wave Hub impact on seabed and shoreline processes report, Tech. rep.

Capobianco, M., Larson, M., Nicholls, R.J. and Kraus, N.C., 1997. Depth of closure: a contribution to the reconciliation of theory, practice and evidence, *Proc. Coastal Dynamics'97*, Plymouth, ASCE, New York: 506-515.

Grant, W.D., and Madsen, O.S., 1982. Movable bed roughness in unsteady oscillatory flow, *J. Geoph. Res.*, 87: 469-481.

Hallermeier, R.J. 1978. Uses for a calculated limit depth to beach erosion, *Proc. 16th Coastal Engineering*, ASCE, Hamburg, 1493–1512.

Hallermeier, R.J., 1981. A profile zonation for seasonal sand beaches from wave climate, *Coastal Engineering*, 4: 253-277.

Hartman, M. and Kennedy, A.B., 2016. Depth of closure over large regions using airborne bathymetric lidar, *Marine Geology,* 379: 52-63.

Hinton, C. and Nicholls, R. J., 1998. Spatial and Temporal Behaviour of Depth of Closure Along the Holland Coast, *26th International Conference on Coastal Engineering*, 2913-2925.

Kraus, N.C., Larson, M. and Wise, R., 1998. Depth of closure in beach fill design, *Proceedings 12th National Conference on Beach Preservation Technology*, Florida Shore and Beach Preservation Association, 271-286.

Masselink G., Scott T., Poate T., Russell P., Davidson M. and Conley D., 2015.The extreme 2013/2014 winter storms: hydrodynamic forcing and coastal response along the southwest coast of England, *Earth Surface Processes and Landforms*, n/a-n/a.

May, V.J. and Hansom, J.D., 2003. *Coastal Geomorphology of Great Britain, geological Edition*, Joint Nature Conservation Committee, Peterborough, U. K.

Nicholls, R.J., Birkemeier, W.A. and Lee, G., 1998a. Evaluation of depth of closure using data from Duck, NC, USA, *Marine Geology*, 148 (3-4): 179 - 201.

Nicholls, R.J., Larson, M., Capobianco, M. and Birkemeier, W. A., 1998b. Depth of closure: Improving understanding and prediction, *Proceedings of the Coastal Engineering Conference,* 3: 2888 - 2901.

Nielsen, P., 1981. Dynamics and geometry of wave-generated ripples, *J. Geophys. Res.*, 86: 6467 – 6472.

Ortiz, A.C., Ashton and A.D., 2016. Exploring shoreface dynamics and a mechanistic explanation for a morphodynamic depth of closure, *Journal of Geophysical Research F: Earth Surface*, 121 (2): 442-464.

Peters, S.E. and Loss, D.P., 2012. Storm and fair-weather wave base: A relevant distinction? *Geology*, 40(6): 511‑514.

Roy, P.S. and Thorn, B.G., 1981. Late quaternary marine deposition in New South Wales and southern Queensland – An evolutionary model, *Journal of the Geological Society of Australia*, 28: 417-489.

Scott, T., Masselink, G. and Russell, P., 2011. Morphodynamic characteristics and classification of beaches in England and Wales, *Marine Geology,* 286 (1-4): 1 - 20.

Soulsby, R.L., 1997. *Dynamics of marine sands: a manual for practical applications*, Thomas Telford, London.

Thieler, E.R., Pilkey, O.H., Clearly, W.J. and Schwab W.C., 2001. Modern sedimentation on the shoreface and inner continental shelf at Wrightsville Beach, North Carolina, USA, J. Sediment. Res., 71(6): 958‑970.